

KGMM: A K-means Clustering Approach to Gaussian Mixture Modeling for Score Function Estimation

Ludovico T Giorgini^{a,*}, Tobias Bischoff^b, Andre N Souza^c

^a*Department of Mathematics, MIT, Cambridge, MA, USA*

^b*Aeolus Labs, San Francisco, CA, USA*

^c*Department of Earth, Atmospheric, and Planetary Sciences, MIT, Cambridge, MA, USA*

Abstract

We propose a hybrid method for accurately estimating the score function—the gradient of the logarithm of a system’s steady-state probability density function—using Gaussian Mixture Model (GMM) in conjunction with a bisecting K-means clustering step. Our approach, which we call KGMM, offers a systematic way to combine statistical density estimation with a neural-network-based interpolation of the score, leveraging the strengths of both. We demonstrate its ability to accurately reconstruct the long-time statistical properties of several paradigmatic systems, including lower-dimensional potential systems and chaotic Lorenz-type models. Numerical experiments show that KGMM yields robust estimates of the score function, even for small values of the covariance amplitude in the GMM, where the standard GMM methods tend to fail because of noise amplification. These accurate estimates allow us to build effective stochastic reduced-order models that reproduce the invariant measures of the target dynamics.

1. Introduction

The score function, defined as the gradient of the logarithm of a system’s steady-state probability density function, is a fundamental quantity in statistical physics, dynamical systems, and machine learning. It underpins key theoretical frameworks such as the Generalized Fluctuation-Dissipation Theorem (GFDT) [1, 2, 3, 4, 5], which links spontaneous fluctuations to system responses, and plays a crucial role in generative modeling [6], parameter estimation [7], and causal inference [8]. Crucially, knowledge of the score function provides insights into the dynamical features of a system without requiring explicit knowledge of its governing equations. Instead, it can be inferred from statistical properties, which are often more accessible in experimental and numerical settings [9, 10, 11, 12, 13].

Accurate and efficient estimation of the score function remains a formidable challenge, particularly in high-dimensional systems. Gaussian Mixture Models (GMMs) are widely used to approximate complex probability distributions due to their flexibility and well-established probabilistic framework [14]. In a GMM, the probability density function is modeled as a weighted sum of Gaussian components, where the mean vectors of the Gaussians are chosen to span the state space explored by the underlying dynamical system.

A critical aspect of using GMMs is the selection of the covariance matrix amplitude for each Gaussian component. Larger covariance amplitudes result in a smoother estimated invariant density because the Gaussian kernel effectively averages out local fluctuations. However, this smoothing comes at a cost: the estimated density is perturbed relative to the true invariant density, as the convolution with the Gaussian kernel tends to blur finer details of the distribution. Conversely, smaller covariance amplitudes produce an invariant density estimate that more closely resembles the true distribution. Yet, the reduction in smoothing increases the noise level in the estimate, which is particularly problematic when differentiating the density to compute the score function. Here, even slight noise amplification can lead to significant inaccuracies in the gradient estimates. Although increasing the number of Gaussian mixture components can help mitigate these issues by providing a more detailed approximation, this solution introduces additional computational burdens and an elevated risk of overfitting [15].

Recent advancements in score-based generative modeling [16, 17, 6, 18, 19, 20] offer an alternative strategy by directly training a neural network to approximate the score function via a dataset-wide loss minimization procedure. This method relies on the implicit regularization afforded by the neural network training procedure to define a “smoothed” version of the Gaussian mixture score function. However, this approach is computationally expensive, as the loss function depends on the entire dataset, and there is no guarantee that the learned score function converges to the true underlying gradient field.

In this work, we propose a hybrid approach that leverages both GMM-based statistical estimation and neural network interpolation. Our method first computes the score function at

*Corresponding author

Email addresses: ludogio@mit.edu (Ludovico T Giorgini), sandre@mit.edu (Andre N Souza)

URL: ludogiorgi.github.io (Ludovico T Giorgini), sandreza.github.io (Andre N Souza)

representative points in the state space by combining a bisecting K-means clustering algorithm with GMM. As we will show, this strategy enables the efficient evaluation of a discretized version of the score function by leveraging information from the whole dataset. We then train a neural network to interpolate between these points, ensuring a scalable and efficient reconstruction of the score function while maintaining the statistical robustness of GMM-based estimation. This method combines the advantages of probabilistic density modeling with the flexibility of machine learning, leading to a computationally efficient and precise framework for score function estimation in large datasets.

The article is structured as follows. Section 2 presents the KGMM method, detailing its derivation and advantages over standard GMMs. Section 3 validates KGMM through numerical experiments on potential and chaotic systems, comparing estimated score functions with analytical solutions when available. Section 4 concludes with key findings and future directions.

2. Method

2.1. Motivation

The dynamics of physical systems often exhibit a hierarchical structure in their spatiotemporal evolution, wherein predictable, low-dimensional processes emerge on longer timescales and larger spatial scales, while chaotic, high-dimensional fluctuations dominate at shorter timescales and finer spatial resolutions. In many complex systems, the details of small-scale, fast processes become increasingly irrelevant under coarse-graining transformations and can be effectively replaced by stochastic forcing terms that preserve essential statistical and dynamical properties. This paradigm not only provides a faithful representation of the underlying physics but also enables a significant reduction in the dimensionality of high-dimensional systems, facilitating both analytical tractability and numerical efficiency.

A paradigmatic example of this approach is found in climate physics, where large-scale, slow dynamics, such as ocean circulation and seasonal variations, coexist with small-scale, rapid processes, including turbulent eddies and convective storms. Reduced-order stochastic models provide an effective means of capturing the statistical and dynamical structure of such multi-scale interactions, successfully replicating phenomena like the El Niño-Southern Oscillation (ENSO), monsoonal cycles, and long-range teleconnections, as well as the coupling of climate variables observed in paleoclimate data [21, 22, 23, 24, 25].

Based on observations of a physical system characterized by a steady-state distribution $\rho_S(\mathbf{x})$ and time correlation function $C(t)$, the following Langevin equation is constructed to inherently reproduce these properties:

$$\dot{\mathbf{x}}(t) = \Sigma \Sigma^T \nabla \ln \rho_S(\mathbf{x}) + \sqrt{2} \Sigma \xi(t), \quad (1)$$

where $\xi(t)$ is a vector of independent Gaussian white noise process, and the covariance matrix Σ is chosen to match the

time-correlations of the observed data. This formulation ensures that ρ_S remains invariant under the corresponding Fokker-Planck operator,

$$\mathcal{L}_{FP} \rho_S = 0, \quad \text{with} \quad \mathcal{L}_{FP} f = -\nabla \cdot (\Sigma \Sigma^T \nabla \ln \rho_S f) + \nabla \cdot (\Sigma \Sigma^T \nabla f), \quad (2)$$

which governs the evolution of probability density in the reduced-order model.

The key observation here is that the deterministic drift term in the Langevin equation (1) is determined by the score function, $\nabla \ln \rho_S(\mathbf{x})$, which encapsulates the structure of the underlying dynamical system. Knowledge of this drift term provides insight into the statistical and dynamical properties of the observed system, including the ability to quantify how the system responds to external perturbations [26]. In the next section, we will show how, by leveraging statistical estimation techniques alongside machine learning approaches, it becomes possible to reconstruct this fundamental quantity with high fidelity, offering new avenues for the systematic derivation of stochastic models in complex dynamical systems.

2.2. Derivation of the Score Function

A Gaussian Mixture Model (GMM) models a probability density function as a weighted sum of Gaussian components:

$$p(\mathbf{x}) = \sum_{k=1}^K w_k \mathcal{N}(\mathbf{x} | \boldsymbol{\mu}_k, \Sigma_k), \quad (3)$$

where w_k denote the weights, $\boldsymbol{\mu}_k$ denote the mean vectors, and the covariance matrices are assumed to be isotropic, i.e. $\Sigma_k = \sigma^2 \mathbf{I}$, with \mathbf{I} the identity matrix. The weights w_k represents the probability associated with each $\boldsymbol{\mu}_k$, indicating the proportion of the dataset that each $\boldsymbol{\mu}_k$ represents. The weights sum to one.

The score function, defined as the gradient of the logarithm of the probability density, is given by:

$$\nabla \ln p(\mathbf{x}) = -\frac{1}{\sigma^2} \sum_{k=1}^K \frac{w_k \mathcal{N}(\mathbf{x} | \boldsymbol{\mu}_k, \sigma^2 \mathbf{I})(\mathbf{x} - \boldsymbol{\mu}_k)}{p(\mathbf{x})}. \quad (4)$$

We now specialize the expression for the score to the case where $K = N$, corresponding to the number of data points. Defining the change of variables

$$\mathbf{z}_k = \mathbf{x} - \boldsymbol{\mu}_k, \quad (5)$$

and taking the limit $N \rightarrow \infty$, we can rewrite Eq. (4) as

$$\nabla \ln p(\mathbf{x}) = -\frac{1}{\sigma^2} \int_{\Omega_\mu} \frac{p(\boldsymbol{\mu}) \mathcal{N}(\mathbf{z} | \mathbf{0}, \sigma^2 \mathbf{I})}{p(\mathbf{x})} \mathbf{z} d\boldsymbol{\mu}, \quad (6)$$

where the integral is carried out over the whole phase space Ω_μ and $p(\boldsymbol{\mu}) = \rho_S(\boldsymbol{\mu})$, that is the invariant measure of the dynamical system. Let's now define

$$p(\mathbf{z}) = \mathcal{N}(\mathbf{z} | \mathbf{0}, \sigma^2 \mathbf{I}) \quad (7)$$

the probability density function of \mathbf{z} and let's rewrite the probability density function of $\boldsymbol{\mu}$ as

$$p(\boldsymbol{\mu}) = p(\boldsymbol{\mu} + \mathbf{z} | \mathbf{z}) = p(\mathbf{x} | \mathbf{z}). \quad (8)$$

Thus, we can express

$$\frac{p(\mathbf{x} | \mathbf{z})p(\mathbf{z})}{p(\mathbf{x})} = p(\mathbf{z} | \mathbf{x}). \quad (9)$$

Substituting this back into the score expression, we obtain

$$\nabla \ln p(\mathbf{x}) = -\frac{1}{\sigma^2} \int_{\Omega_{\mu}} p(\mathbf{z} | \mathbf{x}) \mathbf{z} d\mathbf{z} = -\frac{1}{\sigma^2} \mathbb{E}[\mathbf{z} | \mathbf{x}]. \quad (10)$$

We evaluate the score function at a finite set of points in phase space. To this end, we partition the phase space into N_C clusters $\{\Omega_j\}_{j=1}^{N_C}$ with corresponding centroids \mathbf{C}_j .

The number of clusters, N_C , introduces a critical performance trade-off. A larger N_C improves the spatial resolution of score function estimates by allowing finer-grained cluster subdivisions that better approximate the local gradient structure near the centroids. However, an excessively large N_C reduces the number of samples per cluster, which amplifies statistical noise in the averaged score estimates, while too few clusters risk oversmoothing the score function—particularly in regions of rapid gradient variation. Moreover, in high-dimensional spaces, the exponential growth of the feature space necessitates a careful increase in N_C with the dimension d ; finer subdivisions become essential to capture local variations without loss of information. Empirically, one may adopt a scaling rule of the form

$$N_C \propto \sigma^{-d}, \quad (11)$$

where σ denotes the covariance amplitude. This scaling ensures that each cluster is sufficiently homogeneous for accurate estimation while still containing enough data points, thereby balancing spatial resolution with statistical reliability. Optimal N_C is ultimately guided by both the characteristic length scales of the underlying density, $\rho_S(\mathbf{x})$, and the intrinsic dimensionality of the dataset.

We use for the clustering procedure the bisecting K-means clustering algorithm of [27]. The bisecting k -means algorithm was selected over density-based methods such as DBSCAN [28] due to its deterministic partitioning behavior and scalability in high-dimensional spaces. While DBSCAN excels at identifying arbitrarily shaped clusters with minimal parameter tuning, its reliance on neighborhood density calculations becomes computationally prohibitive for large N -dimensional datasets. In contrast, bisecting k -means achieves a time complexity of $\mathcal{O}(N \ln N_C)$ through iterative binary splits, thus avoiding the pairwise distance comparisons of $\mathcal{O}(N^2)$ inherent to density-based approaches. This hierarchical strategy effectively preserves cluster coherence in sparse regions while maintaining linear scalability with dataset size—an essential advantage when processing large samples.

The average score within each cluster is then given by

$$\nabla \ln p(\mathbf{C}_j) \approx -\frac{1}{\sigma^2} \int_{\Omega_j} \mathbb{E}[\mathbf{z} | \mathbf{x}] p(\mathbf{x}) d\mathbf{x}. \quad (12)$$

This integral is approximated by summing over sample values of \mathbf{x} drawn from $p(\mathbf{x})$ within each cluster, and normalizing by

the number of samples in the cluster, denoted N_C^j . In our implementation, we generate these sample points by drawing N samples using

$$\mathbf{x}_i = \boldsymbol{\mu}_i + \sigma \mathbf{z}_i, \quad (13)$$

where $\boldsymbol{\mu}_i$ are the data points and \mathbf{z}_i are random variables drawn from $\mathcal{N}(\mathbf{0}, \mathbf{I})$. Thus, the discretized form of the K-means cluster-averaged GMM score function (KGMM) becomes

$$\nabla \ln p(\mathbf{C}_j) \approx -\frac{1}{N_C^j \sigma} \sum_{i: \mathbf{x}_i \in \Omega_j} \mathbf{z}_i = \frac{\mathbf{q}_j}{\sigma}. \quad (14)$$

This procedure can be iterated by repeatedly generating new samples \mathbf{x}_i using the same data points $\boldsymbol{\mu}_i$ along with newly drawn noise vectors \mathbf{z}_i . Subsequently, a neural network is employed to interpolate between the computed cluster-wise estimates $\nabla \ln p(\mathbf{C}_j)$, yielding a continuous approximation of the score function. The neural network \mathbf{q}_θ is trained to minimize the following loss function:

$$\mathcal{L}(\theta) = \frac{1}{N_C} \sum_{k=1}^{N_C} \|\mathbf{q}_\theta(\mathbf{C}_k) - \mathbf{q}_k\|_2^2, \quad (15)$$

where \mathbf{q}_k is our cluster-wise estimate of $-\mathbb{E}[\mathbf{z} | \mathbf{x}]$ with \mathbf{x}, \mathbf{z} defined in Eq. (13).

The complete procedure is summarized in Algorithm 1.

Algorithm 1 KGMM Score Function Estimation

Require: Dataset $\{\boldsymbol{\mu}_i\}_{i=1}^N$, number of clusters N_C , noise level σ , convergence threshold α

- 1: Initialize k-means clustering to partition $\{\boldsymbol{\mu}_i\}$ into $\{\Omega_k\}_{k=1}^{N_C}$ with centroids $\{\mathbf{C}_k\}$
 - 2: **repeat**
 - 3: **for** $i = 1$ to N **do**
 - 4: Generate noise $\mathbf{z}_i \sim \mathcal{N}(\mathbf{0}, \mathbf{I})$
 - 5: Compute perturbed point $\mathbf{x}_i = \boldsymbol{\mu}_i + \sigma \mathbf{z}_i$
 - 6: Assign \mathbf{x}_i to cluster Ω_k
 - 7: **end for**
 - 8: **for** $k = 1$ to N_C **do**
 - 9: Compute $\mathbf{q}_k = -\frac{1}{|\Omega_k|} \sum_{i \in \Omega_k} \mathbf{z}_i$
 - 10: **end for**
 - 11: **until** Convergence criterion $\|\mathbf{q}_k^{(t)} - \mathbf{q}_k^{(t-1)}\| < \alpha$ for all k
 - 12: Train neural network parameters θ by minimizing loss $\mathcal{L}(\theta)$ in Eq. (15)
-

2.3. Comparison between KGMM and GMM score function

In this subsection, we compare the score function obtained via the standard GMM approach and the one using the proposed KGMM algorithm, highlighting how KGMM remains accurate even for small covariance amplitudes σ . To illustrate the differences, we consider the one-dimensional system

$$\dot{x}(t) = x - x^3 + \sqrt{2}\xi(t), \quad (16)$$

with $\xi(t)$ delta-correlated Gaussian white noise. This system has the exact score function $s(x) = x - x^3$ and density $\rho \propto e^{-U}$, where $U(x) = (1 - x^2)^2/4$.

We use $N = 10^5$ independent samples of the distribution ρ , denoted by μ_ω , and fit a Gaussian mixture model of the form

$$\rho(x) = \frac{1}{N} \sum_{\omega=1}^N \frac{1}{\sqrt{2\pi\sigma^2}} e^{-\frac{(x-\mu_\omega)^2}{2\sigma^2}}. \quad (17)$$

The corresponding GMM score function for various choices of σ is

$$\nabla \ln \rho(x) = \frac{\sum_{\omega=1}^N (\mu_\omega - x) e^{-\frac{(x-\mu_\omega)^2}{2\sigma^2}}}{\sigma^2 \sum_{\omega=1}^N e^{-\frac{(x-\mu_\omega)^2}{2\sigma^2}}}. \quad (18)$$

To apply KGMM, we then draw N samples of a random normal variable Z_ω , $\omega = 1, \dots, N$, and construct

$$x_\omega = \mu_\omega + \sigma Z_\omega. \quad (19)$$

We formulate the joint density (x, z) , cluster each x_ω into $K \approx 30$ clusters via K-means, assign the same cluster of x_ω to z_ω , average each z_ω over a cluster and divide by $-\sigma$, ultimately learning a discrete approximation of the score function that is then interpolated by a neural network. This describes only one iteration of Algorithm 1 since we only perturb each data point with noise once. See Figure 1 for an illustration of this procedure for various choices of σ . More generally we would construct $x_{\omega\omega'} = \mu_\omega + \sigma z_{\omega'}$ and iterate both $\omega \in \{1, \dots, N\}$ and $\omega' \in \{1, \dots, N \times M\}$, for some natural number $M \geq 1$, until we have a converged estimate of the score.

When the amplitude of the covariance matrix σ in standard GMM is decreased, we get a noisier and noisier estimation of the score function because the differentiation becomes more sensitive to data fluctuations. By contrast, our KGMM algorithm leverages the additional cluster-based regularization and the subsequent neural network interpolation to remain stable for small values of σ , achieving good agreement with the true score function.

3. Results

We tested the proposed KGMM score estimation algorithm on four different stochastic reduced-order models relevant in climate science. For each system, we constructed the score function using KGMM and compared it with its analytic expression when available. We also used the estimated KGMM score function to generate stochastic trajectories by integrating the Eq. (1):

$$\dot{x}(t) = \Sigma \Sigma^T \nabla \ln \rho_S(x) + \sqrt{2} \Sigma \xi(t), \quad (20)$$

where $\xi(t)$ is a vector of independent delta-correlated Gaussian white noise processes. We used $\Sigma = I$. We evaluated the steady-state distributions of these generated trajectories and compared them with those obtained from the observed data to verify whether the KGMM-estimated score function correctly reproduces the invariant measure of the underlying dynamical system.

Each system was simulated over a time interval $T \in [0, 10^5 t_d]$, where t_d denotes the decorrelation time of the system. These datasets were subsequently used to train the KGMM-based score function estimation method. For each system, we employed a three-layer neural network with 128 and 64 neurons in the first and second hidden layers, respectively. We used the Swish activation function between the first two layers, and a linear activation function for the output layer.

3.1. Reduced Triad Model

The triad model, as detailed in [29], serves as a fundamental representation of nonlinear energy exchanges among interacting modes in turbulent systems. By leveraging timescale separation techniques, this system can be effectively reduced from its three-dimensional formulation to a one-dimensional stochastic differential equation, capturing the essential low-frequency behavior while parameterizing unresolved fast-scale interactions.

The resulting reduced-order stochastic differential equation takes the form:

$$\dot{x}(t) = F + ax(t) + bx^2(t) - cx^3(t) + \sigma_1 \xi_1(t) + \sigma_2(x) \xi_2(t), \quad (21)$$

where the deterministic drift coefficients and external forcing term are defined as:

$$\begin{aligned} a &= -1.809, & b &= -0.0667, & c &= 0.1667, \\ A &= 0.1265, & B &= -0.6325, & F &= \frac{AB}{2}, \end{aligned} \quad (22)$$

and the noise amplitudes are given by:

$$\sigma_1 = 0.0632, \quad \sigma_2(x) = A - Bx. \quad (23)$$

An analytical expression for the score function of this model is available:

$$s(x) = 2 \frac{\frac{AB}{2} + (a - B^2)x + bx^2 - cx^3}{\sigma_1^2 + \sigma_2^2(x)}, \quad (24)$$

where the denominator reflects the additive and multiplicative noise contributions. We used $\sigma = 0.01$ and $N_C = 343$ inside Algorithm 1.

In Fig. 2 we compared the score function and the steady-state distribution estimated with the KGMM algorithm with their ground truths. As shown in the figure, the KGMM-estimated score function closely matches the analytical expression. Additionally, integrating Eq. (1) with the KGMM score function as the drift term successfully reconstructs the steady-state distribution and reproduces key statistical properties of the original system.

3.2. Two-Dimensional Asymmetric Potential System

The two-dimensional asymmetric potential system is governed by the stochastic differential equation:

$$\dot{x}(t) = -\nabla U(x) + \sqrt{2} \xi(t), \quad (25)$$

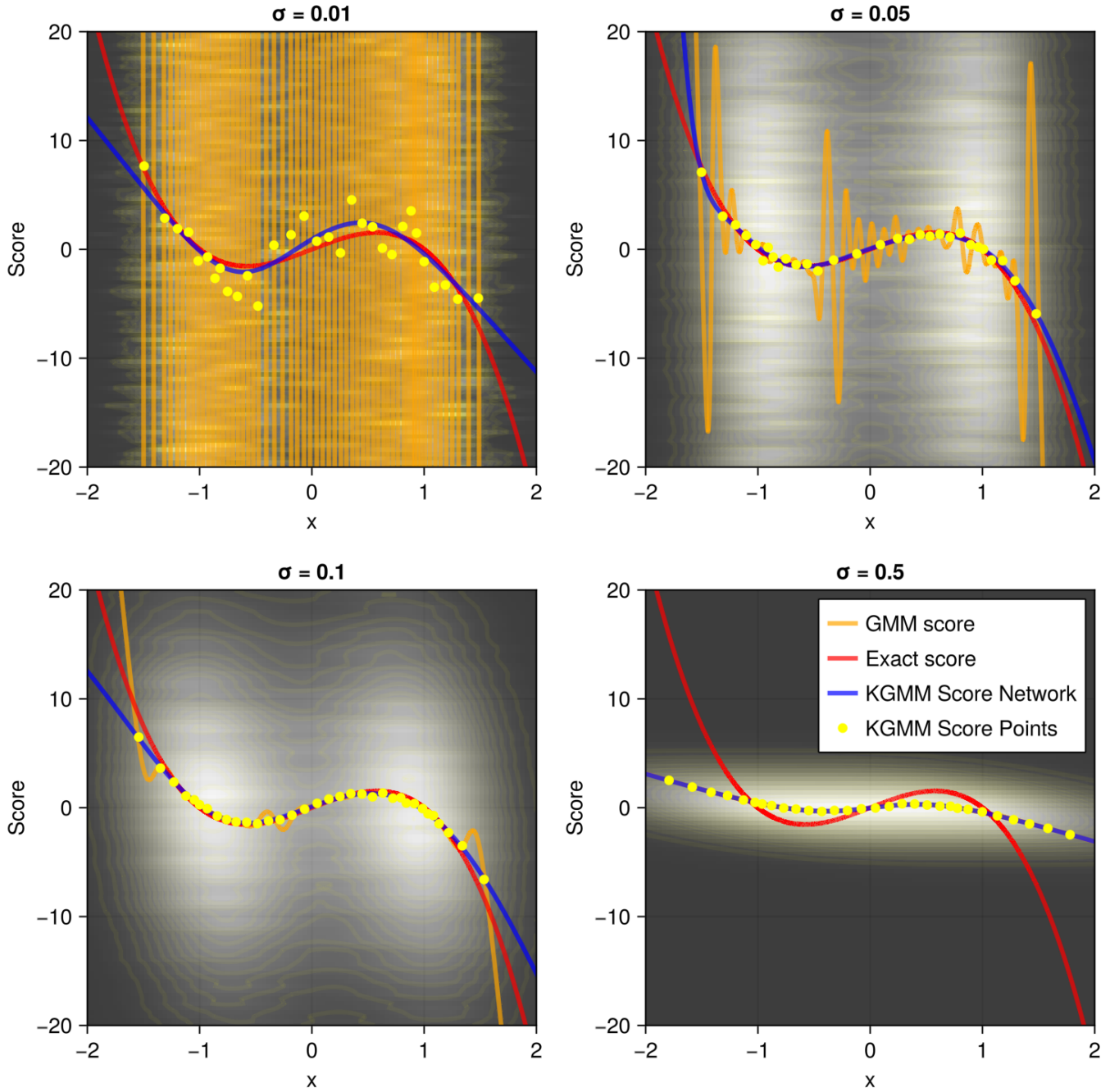


Figure 1: Comparison for different values of σ between the score function obtained through the standard GMM (orange curve) and the one (blue curve) obtained by interpolating the discrete values of the KGMM score function (yellow points). Note that for small σ , the standard GMM curve becomes significantly noisier, whereas the KGMM approach preserves a close agreement with the true score (red curve). Each panel's white and black background represents the joint distribution of $(x_\omega, -z_\omega/\sigma)$, $\omega \in \{1, \dots, N\}$. Fixing a value of x and computing the expected value of the resulting conditional density yields the value of the yellow points.

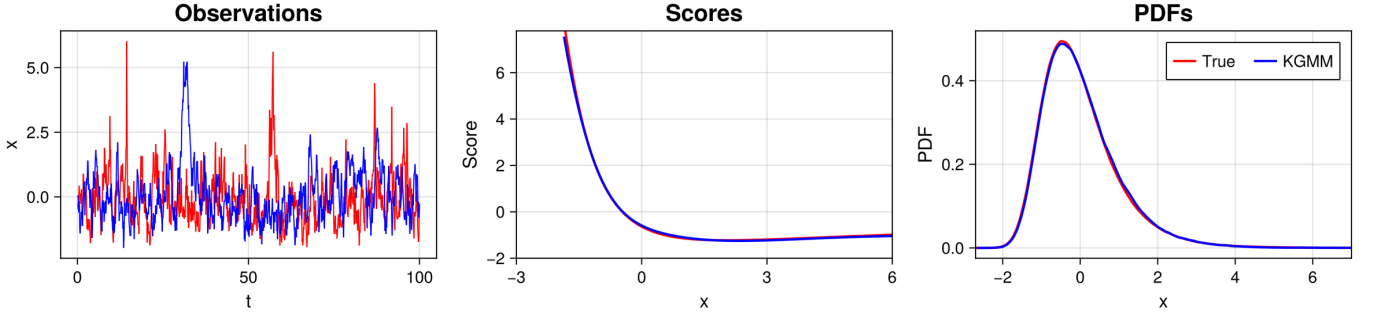


Figure 2: Reduced triad model (Eq. (21)). **Left:** Comparison between trajectories obtained by integrating Eq. (21) (True) and Eq. (1) using the KGMM score function (KGMM). **Center:** Comparison between the KGMM-estimated score function and its analytical expression given by Eq. (24). **Right:** Comparison between the observed steady-state distribution and the one obtained from integrating Eq. (1) using the KGMM score function.

where the potential function $U(\mathbf{x})$ is given by:

$$U(\mathbf{x}) = (x_1 + A_1)^2(x_1 - A_1)^2 + (x_2 + A_2)^2(x_2 - A_2)^2 + B_1 x_1 + B_2 x_2. \quad (26)$$

The coefficients used in our study are:

$$A_1 = 1.0, \quad A_2 = 1.2, \quad B_1 = 0.6, \quad B_2 = 0.3. \quad (27)$$

The corresponding score function is defined as:

$$s(\mathbf{x}) = -\nabla U(\mathbf{x}). \quad (28)$$

We used $\sigma = 0.05$ and $N_C = 721$ inside Algorithm 1.

This model describes an asymmetric potential landscape typical of systems exhibiting multistability, a feature often observed in climate models where multiple stable states can exist [30]. The goal of our analysis is to compare the KGMM-estimated score function with the true score function and assess the accuracy of the reconstructed probability densities.

Figure 3 shows that the KGMM-estimated score function closely matches the analytical score function near the potential minima, where the majority of the observed data points are concentrated. Additionally, the probability density functions obtained using the KGMM-estimated score function agree well with those computed from direct observations.

However, discrepancies between the two score functions are observed in regions far from the potential minima. This deviation arises due to the scarcity of observed data points in these regions, leading to errors in the KGMM-based reconstruction of the score function.

3.3. Stochastic Lorenz 63 Model

The Lorenz 63 system [31] is a classical model for atmospheric convection, encapsulating key features of chaotic behavior in climate dynamics. Unlike the previous two models, the Lorenz 63 system is inherently chaotic. To capture the influence of unresolved processes occurring at shorter timescales, we consider a stochastic extension of the Lorenz 63 system by incorporating a noise term:

$$\begin{aligned} \dot{x}(t) &= \sigma(y(t) - x(t)) + \sigma_\xi \xi_1(t), \\ \dot{y}(t) &= x(t)(\rho - z(t)) - y(t) + \sigma_\xi \xi_2(t), \\ \dot{z}(t) &= x(t)y(t) - \beta z(t) + \sigma_\xi \xi_3(t), \end{aligned} \quad (29)$$

where $\xi_1(t)$, $\xi_2(t)$, and $\xi_3(t)$ are independent Gaussian white noise processes with unit variance. The coefficients used in our study are:

$$\sigma = 10.0, \quad \rho = 28.0, \quad \beta = \frac{8}{3}, \quad \sigma_\xi = 5.0. \quad (30)$$

We used $\sigma = 0.05$ and $N_C = 761$ inside Algorithm 1.

When comparing the trajectory of the original (chaotic) Lorenz 63 system with the trajectory obtained by integrating the corresponding Langevin equation (1) using the KGMM-estimated score function, the time evolution at short timescales can look qualitatively very different. This occurs because the deterministic details in the original chaotic system generate specific trajectories that are highly sensitive to initial conditions, whereas the Langevin approach encodes the steady-state behavior through noise-driven dynamics and does not preserve the exact local chaotic structure. Nevertheless, on longer timescales, the two systems share the same invariant measure, as the KGMM score function accurately reproduces the statistical properties observed in the data.

As shown in Fig. 4, the KGMM-estimated score function successfully reconstructs the steady-state probability distributions of the system. Despite the short-timescale trajectory differences, the long-term statistical agreement demonstrates the robustness of the KGMM approach in capturing the essential invariant features of a chaotic system.

3.4. Stochastic Lorenz 96 Model

The Lorenz 96 model [32], is a paradigmatic system for studying multiscale chaotic dynamics, originally designed as a simplified model of atmospheric circulation. It consists of a set of slow variables, x_k , which evolve on a longer timescale, coupled to a set of fast variables, $y_{k,j}$, representing small-scale turbulent fluctuations. To account for unresolved processes occurring on timescales even shorter than those explicitly modeled, we consider a stochastic extension of the system:

$$\frac{dx_k}{dt} = -x_{k-1}(x_{k-2} - x_{k+1}) - \nu x_k + F + c_1 \sum_{j=1}^{N_j} y_{k,j} + \sigma_\xi \xi_k(t), \quad (31)$$

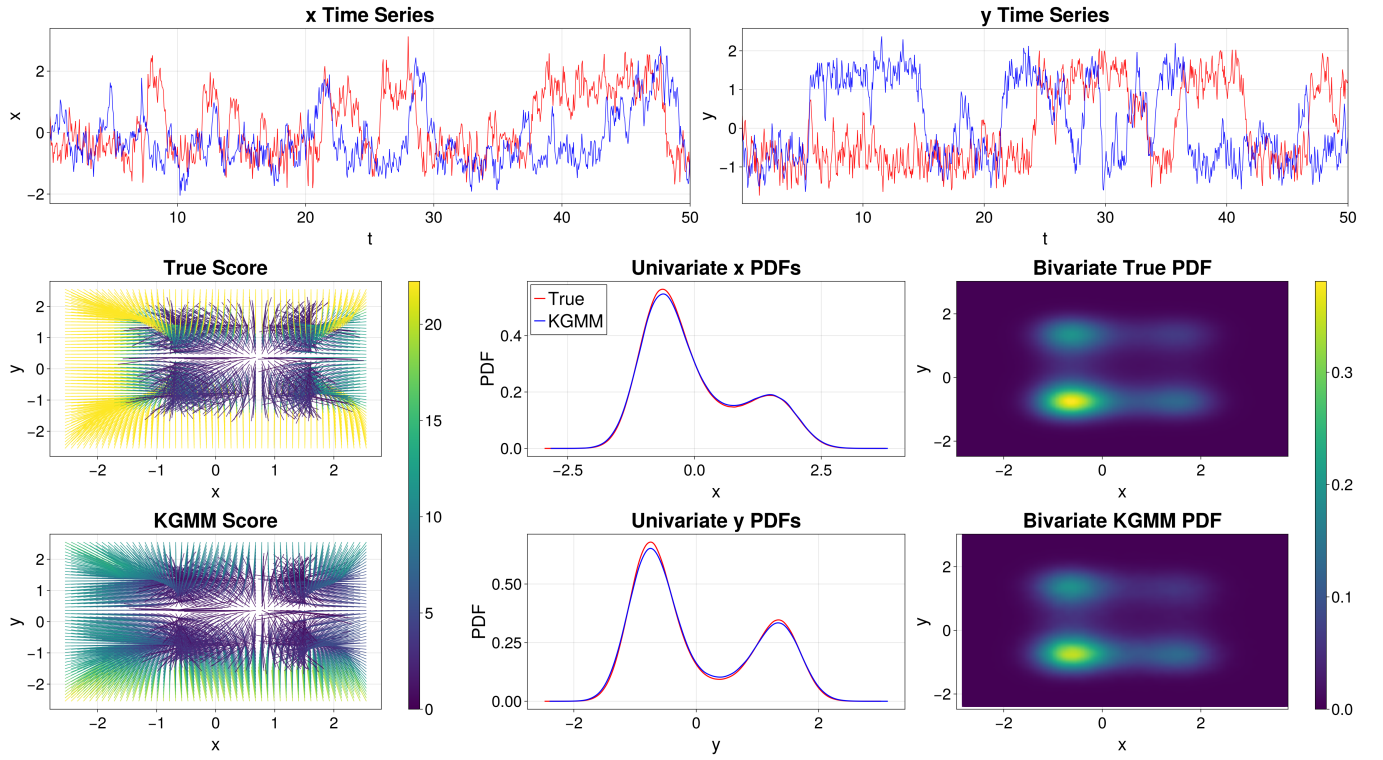


Figure 3: **Two-dimensional asymmetric potential system.** **First row:** Comparison between trajectories obtained by integrating Eq. (26) (True) and Eq. (1) using the KGMM score function (KGMM). **Second and third rows, first column:** The force field of the true score function (top) and the force field of the KGMM-estimated score function (bottom). **Second and third rows, second column:** Comparison between the observed univariate PDFs (red) and those obtained by integrating Eq. (25) with the KGMM-estimated score function (blue). **Second and third rows, third column:** Comparison between the observed bivariate probability density (top) and the reconstructed density using the KGMM-based score function (bottom).

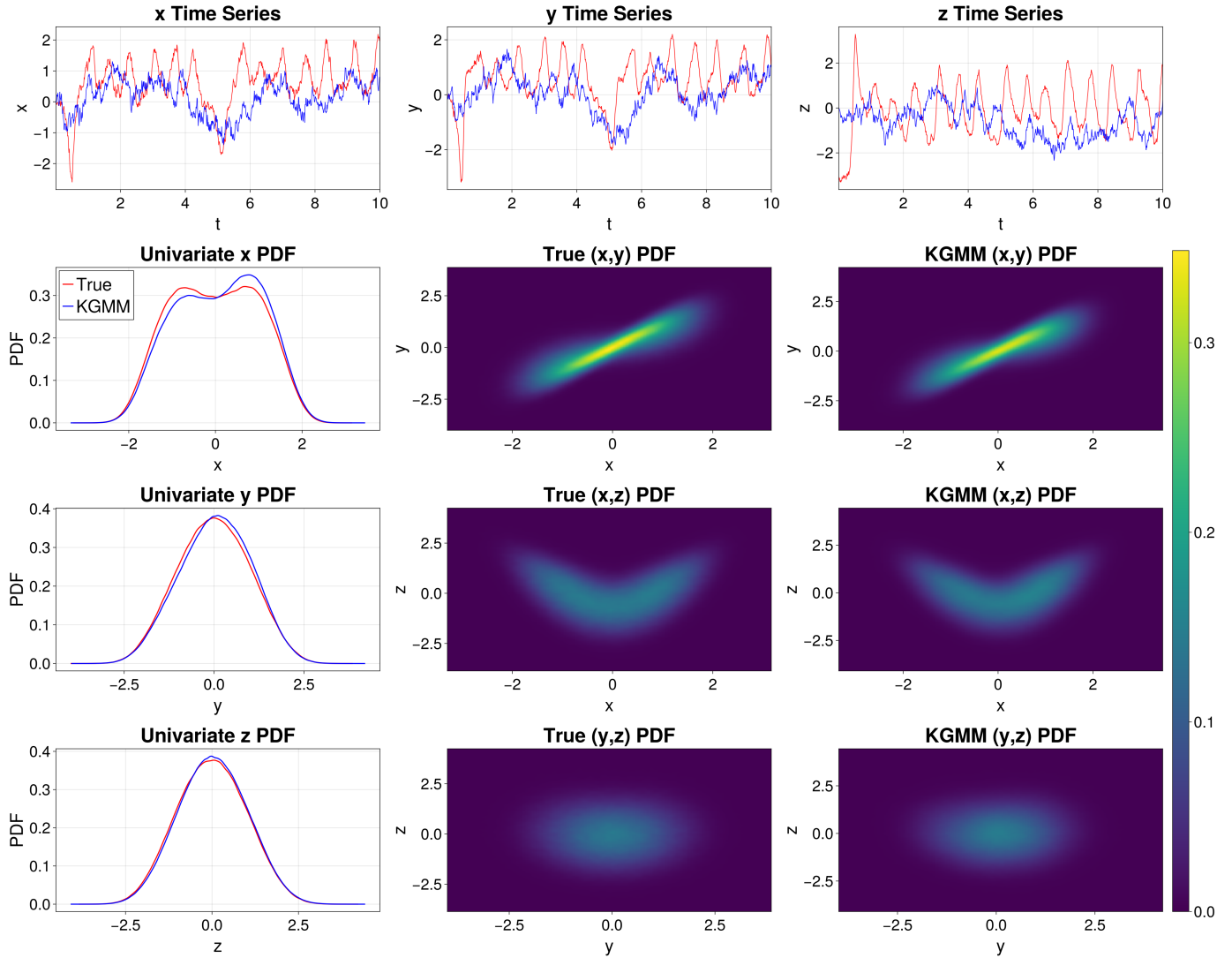


Figure 4: **Lorenz 63 system.** **First row:** Comparison between trajectories obtained by integrating Eq. (29) (True) and Eq. (1) using the KGMM score function (KGMM). **Second to fourth rows, first column:** Comparison between the observed univariate PDFs (red) and those obtained integrating the Langevin equation using the KGMM-estimated score function (blue). **Second to fourth rows, second and third columns:** Comparison between the observed bivariate PDFs (left) and those obtained using the KGMM-based score function (right).

$$\frac{dy_{k,j}}{dt} = -cb y_{k,j+1}(y_{k,j+2} - y_{k,j-1}) - cv y_{k,j} + c_1 x_k + \sigma \xi_{k,j}(t). \quad (32)$$

Here, $\xi_k(t), \xi_{k,j}(t)$ are uncorrelated Gaussian white noise processes with unit variance, representing the effect of high-frequency fluctuations not explicitly resolved. The model parameters are chosen as follows:

$$\begin{aligned} F &= 4.0, & \nu &= 1.0, & c &= 10.0, \\ b &= 10.0, & c_1 &= \frac{c}{b} = 1.0, & \sigma &= 0.2. \end{aligned} \quad (33)$$

This formulation naturally introduces three distinct timescales into the system. The shortest timescale is associated with the stochastic forcing term, the intermediate timescale corresponds to the chaotic dynamics of the 40-dimensional fast process $\{y_{k,j}\}$, and the longest timescale governs the evolution of the 4-dimensional slow variables $\{x_k\}$. We used $\sigma = 0.05$ and $N_C = 3818$ inside Algorithm 1.

Similar to the Lorenz 63 case, comparing the short-timescale behavior of the original Lorenz 96 trajectories with those obtained by integrating (1) using the KGMM-estimated score function reveals qualitative differences due to the deterministic chaotic nature of the full Lorenz 96 model. However, as time evolves, both the original system and the KGMM-based Langevin model settle into the same statistical regime, sharing the same invariant measure. Due to the symmetries in the system, we present only the trajectory and univariate distribution for a single variable, as the behavior of the remaining variables is statistically equivalent.

The degree of chaos in the Lorenz 96 system depends on the magnitude of the external forcing F and the number of slow variables N_k . For larger values of F and N_k , the system exhibits fully developed turbulence, and its steady-state distribution approaches a multivariate Gaussian. In this study, we focus on an intermediate chaotic regime where the steady-state PDF deviates significantly from a Gaussian distribution. This choice allows us to better assess the ability of the KGMM method to accurately reconstruct non-Gaussian statistical structures, which would be harder to detect in a system where the steady-state distribution is trivially Gaussian.

4. Conclusions

We have presented a hybrid method for estimating the score function by leveraging Gaussian Mixture Models and bisecting K-means clustering (KGMM). Our approach overcomes the noise amplification issues encountered in direct GMM-based methods for small covariance amplitudes and efficiently recovers the long-term statistical properties of both low-dimensional potential systems and chaotic Lorenz-type models. Although the resultant stochastic trajectories may differ in their short-timescale details from those of the original chaotic systems, they converge to the same invariant measures, indicating that KGMM accurately reproduces the essential large-timescale dynamics.

As a future direction, we plan to extend KGMM to higher-dimensional systems, exploring its performance in complex

scenarios with strong multiscale interactions and large state spaces. This will open up new possibilities for data-driven reduced-order modeling in climate science, fluid dynamics, and other areas where accurate score function estimation is crucial for capturing the stochastic behavior and long-term statistics of complex dynamical systems.

References

- [1] U. M. B. Marconi, A. Puglisi, L. Rondoni, A. Vulpiani, Fluctuation-dissipation: Response theory in statistical physics, *Physics Reports* 461 (4-6) (2008) 111–195. doi:10.1016/j.physrep.2008.02.002.
- [2] L. T. Giorgini, K. Deck, T. Bischoff, A. Souza, Response theory via generative score modeling, *Physical Review Letters* 133 (26) (2024) 267302.
- [3] F. C. Cooper, P. H. Haynes, Climate sensitivity via a nonparametric fluctuation–dissipation theorem, *Journal of the Atmospheric Sciences* 68 (5) (2011) 937–953.
- [4] M. Baldovin, F. Cecconi, A. Vulpiani, Understanding causation via correlations and linear response theory, *Physical Review Research* 2 (4) (2020) 043436.
- [5] M. Ghil, V. Lucarini, The physics of climate variability and climate change, *Reviews of Modern Physics* 92 (3) (2020) 035002.
- [6] Y. Song, J. Sohl-Dickstein, D. Kingma, S. Ermon, Score-based generative modeling through stochastic differential equations, in: *International Conference on Learning Representations (ICLR)*, 2021.
- [7] B. W. Silverman, *Density Estimation for Statistics and Data Analysis*, Chapman and Hall/CRC, 1986.
- [8] S. Shimizu, P. Hoyer, A. Hyvärinen, A. Kerminen, A linear non-gaussian acyclic model for causal discovery, *Journal of Machine Learning Research* 7 (2007) 2003–2030.
- [9] F. Falasca, P. Perezhugin, L. Zanna, Data-driven dimensionality reduction and causal inference for spatiotemporal climate fields, *Physical Review E* 109 (4) (2024) 044202.
- [10] L. T. Giorgini, A. N. Souza, D. Lippolis, P. Cvitanović, P. Schmid, Learning dissipation and instability fields from chaotic dynamics, *arXiv preprint arXiv:2502.03456* (2025).
- [11] L. T. Giorgini, A. N. Souza, P. J. Schmid, Reduced markovian models of dynamical systems, *Physica D: Non-linear Phenomena* 470 (2024) 134393.
- [12] A. N. Souza, Representing turbulent statistics with partitions of state space. part 1. theory and methodology, *Journal of Fluid Mechanics* 997 (2024) A1.
- [13] A. N. Souza, Representing turbulent statistics with partitions of state space. part 2. the compressible euler equations, *Journal of Fluid Mechanics* 997 (2024) A2.
- [14] Y. Teh, M. Jordan, M. Beal, D. Blei, Hierarchical dirichlet processes, *Journal of the American Statistical Association* 101 (476) (2006) 1566–1581. doi:10.1198/016214506000000302.
- [15] D. Reynolds, Gaussian mixture models, *Encyclopedia of Biometrics* (2009) 659–663.
- [16] A. Hyvärinen, Estimation of non-normalized statistical models by score matching, *Journal of Machine Learning Research* 6 (2005) 695–709.
- [17] P. Vincent, A connection between score matching and denoising autoencoders, *Tech. Rep. 1358*, Université de Montréal, Department of Computer Science and Operations Research (2011).
- [18] F. Vargas, A. Ovsianas, D. Fernandes, M. Girolami, N. D. Lawrence, N. Nüsken, Bayesian learning via neural schrödinger–föllmer flows, *Statistics and Computing* 33 (1) (2023) 3.
- [19] T. Bischoff, B. Riel, Enhancing score-based sampling methods with ensembles, *arXiv preprint arXiv:2401.17539* (2024).
- [20] R. Schwank, Robust score matching, *arXiv preprint arXiv:2501.05105* (2025).
- [21] A. J. Majda, C. Franzke, B. Khouider, An applied mathematics perspective on stochastic modelling for climate, *Philosophical Transactions of the Royal Society A: Mathematical, Physical and Engineering Sciences* 366 (1875) (2008) 2427–2453.
- [22] N. Chen, Y. Zhang, Rigorous derivation of stochastic conceptual models for the el niño-southern oscillation from a spatially-extended dynamical system, *Physica D: Nonlinear Phenomena* 453 (2023) 133842.

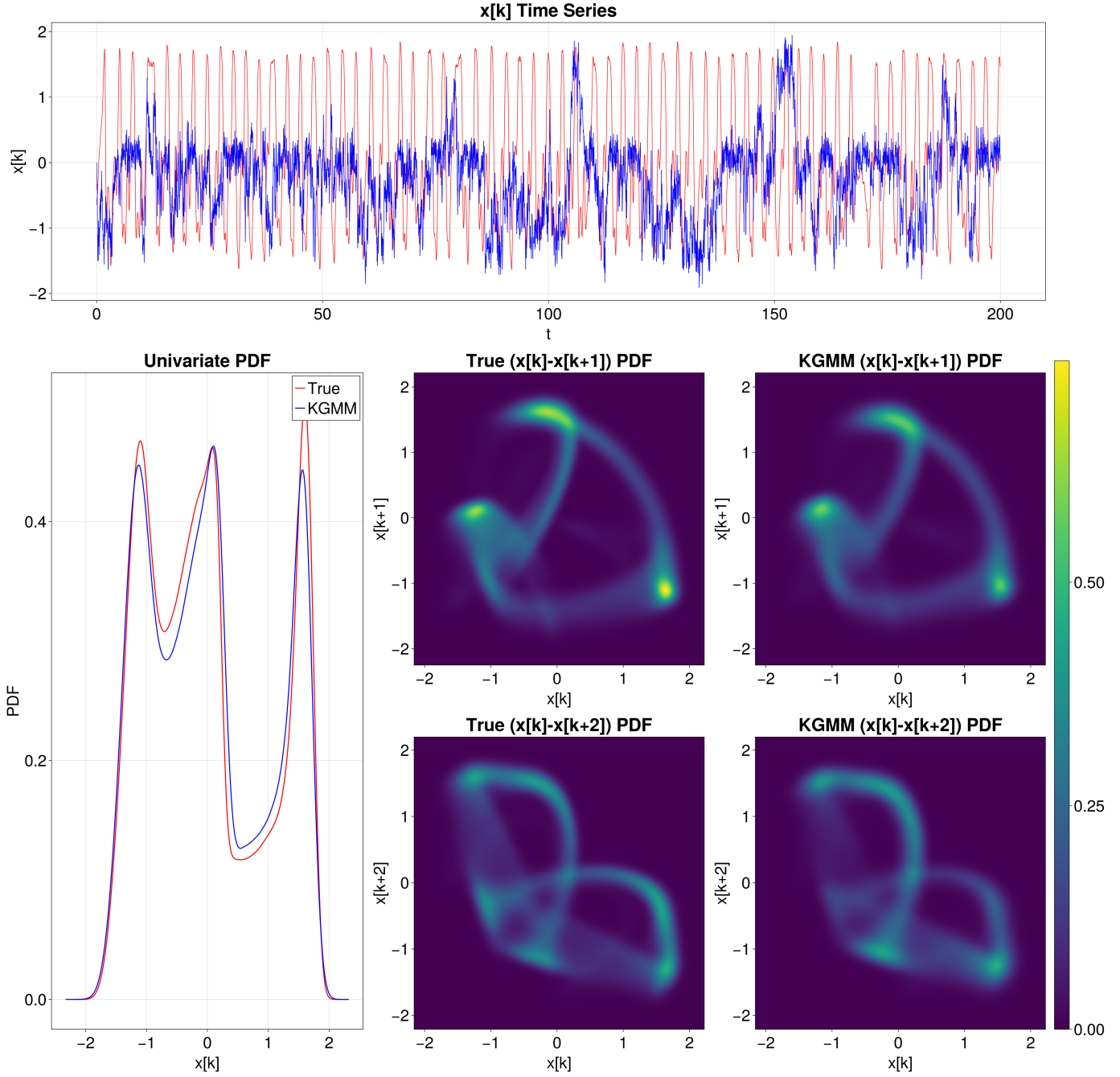


Figure 5: **Lorenz 96 system.** **First row:** Comparison between trajectories obtained by integrating Eq. (32) (True) and Eq. (1) using the KGMM score function (KGMM). **Second row, first column:** Comparison between the observed univariate PDFs (red) and the one obtained integrating the Langevin equation using the KGMM-estimated score function (blue). **Second and third rows, second and third columns:** Comparison between the observed bivariate PDFs (top) and those obtained using the KGMM-based score function (bottom).

- [23] N. D. Keyes, L. T. Giorgini, J. S. Wettlaufer, Stochastic paleoclimatology: Modeling the epica ice core climate records, *Chaos* 33 (9) (2023) 093132.
- [24] L. T. Giorgini, W. Moon, N. Chen, J. Wettlaufer, Non-gaussian stochastic dynamical model for the el niño southern oscillation, *Physical Review Research* 4 (2) (2022) L022065.
- [25] M. Baldovin, F. Cecconi, A. Provenzale, A. Vulpiani, Extracting causation from millennial-scale climate fluctuations in the last 800 kyr, *Scientific Reports* 12 (1) (2022) 15320.
- [26] M. Baldovin, L. Caprini, A. Vulpiani, Handy fluctuation-dissipation relation to approach generic noisy systems and chaotic dynamics, *Physical Review E* 104 (3) (2021) L032101.
- [27] A. N. Souza, S. Silvestri, A modified bisecting k-means for approximating transfer operators: Application to the lorenz equations, arXiv preprint arXiv:2412.03734 (2024).
- [28] M. Ester, H.-P. Kriegel, J. Sander, X. Xu, A density-based algorithm for discovering clusters in large spatial databases with noise, in: *Proceedings of the Second International Conference on Knowledge Discovery and Data Mining*, 1996, pp. 226–231.
- [29] A. J. Majda, B. Gershgorin, Y. Yuan, Low-frequency climate response and fluctuation–dissipation theorems: Theory and practice, *Journal of the Atmospheric Sciences* 67 (2010) 1186–1201.
- [30] G. Margazoglou, T. Grafke, A. Laio, V. Lucarini, Dynamical landscape and multistability of a climate model, *Proceedings of the Royal Society A* 477 (2250) (2021) 20210019.
- [31] E. N. Lorenz, Deterministic nonperiodic flow 1, in: *Universality in Chaos*, 2nd edition, Routledge, 2017, pp. 367–378.
- [32] E. N. Lorenz, Predictability: A problem partly solved, in: *Proc. Seminar on predictability*, Vol. 1, Reading, 1996, pp. 1–18.